An indoor localization system to detect areas causing the freezing of gait in Parkinsonians

Florenc Demrozi*,Vladislav Bragoi*, Federico Tramarin† and Graziano Pravadelli*
*Dept. of Computer Science, Univ. of Verona, Italy, Email: name.surname@univr.it
†Dept. of Management and Engineering, Univ. of Padua, Italy, Email: name.surname@unipd.it

***Abstract*—People affected by the Parkinson's disease are often subject to episodes of Freezing of Gait (FoG) near specific areas within their environment. In order to prevent such episodes, this paper presents a low–cost indoor localization system specifically designed to identify these critical areas. The final aim is to exploit the output of this system within a wearable device, to generate a rhythmic stimuli able to prevent the FoG when the person enters a risky area. The proposed localization system is based on a classification engine, which uses a fingerprinting phase for the initial training. It is then dynamically adjusted by exploiting a probabilistic graph model of the environment.**

***Index Terms*—Fingerprinting, indoor localization, machine learning, probabilistic graph, Parkinson's disease.**

I. Introduction

People affected by the Parkinson's Disease (PD) may experience episodes of FoG, that cause a sudden interruption of walking with a consequent severe risk of falls [1]. FoG episodes frequently happen when the patient approaches so–called *risky areas*, such as visible obstacles in her/his path, areas with different design patterns of the floor, or the traversal of narrow spaces [2]. Rhythmic stimulation by an accompanying person proved to be effective in solving the FoG, allowing the patient to restart the movement [3]. In this context, the design of wearable devices able to automatically recognize the FoG and to provide such a stimulation is a hot research topic. In some implementations, these devices achieved very good accuracy in FoG detection by analyzing data gathered from on-body sensing devices, like, for example accelerometers or ECGs [4], [5]. Conversely, as far as the prevention of FoG episodes is concerned, applications are still at an earlier stage with unsatisfactory results [6].

This paper hence focuses on the problem of FoG prevention. To this aim, a low–cost localization system is defined, which is able to trigger the generation of the aforementioned rhythmic stimuli when it recognizes that the patient is approaching a risky area, thus anticipating the FoG episode. The proposed approach is intended to be used indoor, such as in the patient's house or work environment. The approach requires that the patient wears a device able to provide rhythmic stimuli (e.g. a smart watch or bracelet) and that the environment is equipped with suitable radio–signal emitters, such as Wireless Local Area Network (WLAN) Access Points (APs) or Bluetooth Low Energy (BLE) beacons.

Although localization systems able to provide decimeter-level localization accuracy have already been proposed in the literature, it is worth highlighting that such a high accuracy is typically obtained through auxiliary/modified devices or decentralized computation [7]–[11]. Nonetheless, it is possible to obtain a satisfactory degree of accuracy even with local approaches based on general purpose devices, for example exploiting a probabilistic graph model of the environment, as discussed in [12].

II. Preliminaries

a) Received Signal Strength Indicator (RSSI): it is a measurement, used often in Radio Frequency (RF)–based communication systems, that is related to the power perceived by a receiver. The rationale is that the higher the RSSI value is and the stronger the signal is [13].

b) Fingerprinting: Fingerprinting technique is now considered the state-of-the-art for indoor localization [14]. Within this approach, the available area is divided in Reference Points (RPs). The distance between any two RPs can be maintained either equal or not necessarily equally spaced.. Each RP_k is identified by a couple (x_k, y_k) of Cartesian coordinates and a matrix r_k of RSSI values recorded from the center of RP_k, where, for a generic $rssi_i^j$ element, j represents the RSSI source index (e.g. an AP), and i represents the recording timestamp. For the sake of completeness, the fingerprinting technique is not constrained to use only RSSI values, since other types of data, e.g., magnetic vector, can be associated to each RP, provided they allow to uniquely identify the RP [15].

III. Methodology

From a practical point of view, the proposed approach is based on two main types of devices. On the one hand, smartphones are exploited to carry out RSSI and Magnetic Field Vector (MV) measurements, as well as to execute computations. On the other hand, this proposal needs the availability of emitters of meaningful radio signals, which in turn have to be manageable by the smartphone to extract the RSSI readings. In this work, we hence consider both Wi-Fi AP and BLE beacons. A detailed view of the proposed method is provided in Fig. 1 and described hereafter.

A. Fingerprinting

The first goal is to create a dataset of RSSI measurements and MV values, based on the following three steps.

1) *Subdivide the environment in RPs*
   a) map all risky areas into a set of RPs, not necessarily contiguous;
2) *Set RP information*
   a) its x, y position;
   b) existence of borders in any cardinal direction (e.g., wall on North);

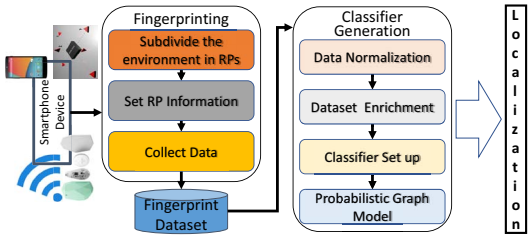

Fig. 1. Schematic view of the proposed methodology.

c) environmental description (e.g., doorway or floor pattern changes);

3) *Collect data*

a) capture RSSI and MV data for each RP.

Columns 1-9 in Table I show how the training set appears after the execution of the aforementioned procedure. Column 1 represents the RP identifier, Columns 2 and 3 are referred to the coordinates of its center c_{xy}, Column 4 reports information about the presence of borders, Column 5 associates the risky area the RP belongs to, Column 6 is the timestamp, Column 7 records the movement direction of the person, finally, Column 8 and Column 9 report the RSSI and MV measurements. Timestamps are in the form *dd:mm:yy:hh:min:sec:ms*. RSSI values are vectors of length n, where n is the number of radio signal emitters placed within the environment.

B. Classifier generation

The classifier generation is characterized by the sequence of operations detailed below.

1) Data normalization: Both the RSSI and the MV datasets have been normalized through a classical min-max feature scaling technique, as shown in Eq. (1).

$$x' = \frac{x - min(x)}{max(x) - min(x)} \tag{1}$$

where x is the original value and x' is the normalized value. This makes the training less sensitive to the scale of features [16].

2) Dataset enrichment: The original fingerprinting dataset is further enriched by associating to each record (i.e., each RP) the result of two elaborations on RSSI and MV measurements (Columns 10 and 11 in Table I), and a grouping label (Column 12 in Table I).

Column 10 categorizes each single RSSI value of Column 8 in classes, according to the following procedure:

a. We apply the k-Means clustering algorithm to the original RSSI data of Column 8, by considering each single $RSSI_i$ measurement, per each timestamp t, uncorrelated with respect to all the others, i.e., we forget that the set of values $RSSI_{[1...n]}$ corresponding to timestamp t, were measured all together when the smartphone was in the same (x, y) position at time t. Given the whole set of RSSI values, k-Means groups them in k clusters, where k is automatically selected to maximize the similarity among the elements belonging to the same cluster.

b. We extract the minimum and maximum RSSI values, min_p and max_p, for each cluster p.

c. We associate each value $RSSI_i$, with $i \in [1 \dots n]$, per each timestamp t, to one of the k clusters according to the following rule: if $min_p \leq RSSI_i \leq max_p$, then $RSSI_i$ is associated to cluster p.

The aforementioned procedure associates a specific cluster to each RSSI values measured with respect to a specific radio–signal emitter in a given instant providing the new categorized RSSI vectors (CRSSI). This maps each RSSI measurement into a set of virtual spatial-temporal locations, not necessarily adjacent neither in space nor in time, that anyway show similar characteristics. An analogous procedure is applied to MV values in Column 9 to obtain the categorized MV classes of Column 11 (CMV).

Finally, the grouping labels in Column 12 are also obtained by using the k-Means clustering algorithm. Nevertheless, k-Means is now applied by adopting, as training set, records composed of both RSSI and MV vectors. In addition, differently from the above procedure, in the training set we preserve the correlation among measurements related to the same position at the same time stamp, i.e. we provide k-Means with RPs instead of single RSSI and MV values. Hence, in this case, the goals is to group RPs into a set of clusters on the basis of the similarity of their respective RSSI and MV measurements.

3) Classifier set up: The proposed localization systems is composed on five classifiers, all of them based on the k-NN machine learning algorithm [17]. They are set up by exploiting in different ways and instants the information reported in Table I, which are extracted according to the procedure described in the previous sections. The first classifier, **C1**, is set up by using the data of Columns 8 and 9 as input and the labels in Column 12 as target classes. Its role is filtering the RPs. Given the RSSI and MV values measured by the smartphone of the person to be localized, C1 associate theses values with one specific target class. Thus, C1 filters the known RPs by restricting the possible location of the person among the RPs belonging to the recognized class.

After **C1** is applied, four different classifiers, **C2**, **C3**, **C4** and **C5** are each one used to select the most representative RP, among the set of RPs returned by **C1**, providing with a narrower set of at most 4 RPs. The datasets for these classifiers are Column 8 for **C2**, Column 10 for **C3**, Column 9 for **C4** and Column 11 for **C5**. For all of them the target classes are represented by RPs returned by C1. Therefore, their choice is based on different aspects that may characterize the actual position of the person. The four RPs so far returned are used in conjunction with a **probabilistic graph model** of the environment, that is generated as reported in the following.

4) Probabilistic graph model: To increase the localization accuracy and to preserve the environment knowledge this paper proposes, as seen in Table I, to record for each RP, possible borders (e.g., walls and furniture) and environment characteristics (e.g., doorway, stairs, floor pattern changes and narrowing of the environment) in one (or more) cardinal directions. Each RP can be seen as a square of side m meters.

Thus, at least one RP is associated to each risky area in the environment, m meters away from it, per each possible direction. The value of the parameter m can be fixed according to the medical experience. In general, a rhythmic stimuli for preventing a FoG episode, while approaching a risky area,

TABLE I
TRAINING DATA FOR THE PROPOSED CLASSIFIERS.

RP ID	Pos. X	Pos. Y	Borders	Description	Timestamp	Direction	$RSSI_{[1\ldots n]}$	$MV_{[x\ y\ z]}$	$CRSSI_{[1\ldots n]}$	$CMV_{[x\ y\ z]}$	Group
1	1	1	North	doorway	t_1	North	[-72 -93 -44 …-56]	[13 9 8]	[3 2 3 …3]	[2 3 1]	l_1
..	..	..	..	..	..	..	..	..	..	..	..
m	23	15	West	narrowing	t_h	West	[-45 -58 -60 …-76]	[5 42 28]	[1 3 3 …2]	[1 3 2]	l_k

should be generated 1.5-2 meters far from it, as the gait speed and the stride length in PD patients is on average, respectively, 1m/s and 1.06m [18]. Different values for m risk to uselessly disturb the patient, if the stimuli is generated too in advance, or being ineffective, if the stimuli is delayed. Figure 2 shows an example of three RPs, where the doorway v_a identifies a risky RP, while v_b and v_c identify adjacent RPs to such a risky RP. Furthermore, colors identify the presence of borders in at least one direction per each RP.

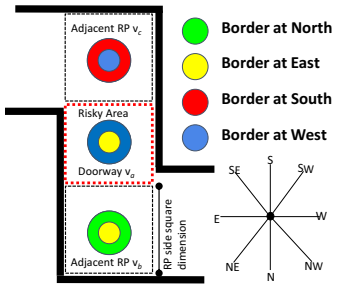

Fig. 2. Example of RPs in proximity of a risky area (doorway).

Hence, we map the characteristics of the environment as a graph model $M = (V, E, P, B, T)$ where:

- $V \in \{V_r \cup V_{ar}\}$ is the set of RPs composed of:
  - V_r: RPs identifying risky areas, e.g. doorways;
  - V_{ar}: identifying RPs adjacent to risky areas;
- $E = \{(v_i, v_j) | v_i, v_j \in V \wedge v_i, v_j \ are\ neighbors\}$ is the set of edges between RPs;
- $P : E \rightarrow [0, 1]$ defines, for each edge $e \in E$, the probability of crossing e;
- $B : V \rightarrow \mathcal{P}(\{N, S, W, E\})$ associates each RP to its set of adjacent borders represented as cardinal points.
- $T : V \rightarrow D$, where D ={pattern change, stairs, doorway, ...}, defines per each RP the characteristic of the environment where the RP is located.

The probability of the edges is first statically computed and then dynamically adjusted during actual localization. Per each edge $e = (v_i, v_j)$, the static value is defined as $1/n$, where n is the number of outgoing edges from v_i, including e, i.e. n counts the possible directions that a person can take starting from v_i, considering that he/she cannot cross obstacles. The maximum number of outgoing edges from v_i is 8 (corresponding to the 8 cardinal points N,NE,E,SE,S,SW,W,NW). During the actual localization, the probability of an edge e is then adjusted by considering the arrival direction of the person, according to the fact that going straightforward for a while is more likely than continuing turning. In practice, if the person reached v_i from South, the probability of edges outgoing from v_i towards RPs located at North, North-Est and North-West with respect to v_i are increased of a quantity $d > 0$. In our experiments we empirically fixed d at $1/3$.

C. Localization

At run-time, the localization phase performs as follows. Let us assume, at time t, the person is located at RP v_i. During walking, the mobile phone perceives radio signals, computes magnetic field vectors and gets movement directions that are periodically provided to the localization system described in the previous section. At time $t + 1$, the perceived RSSI and MV values, after being normalized, are provided to the **C1** classifier. **C1** filters the RPs in the graph model of the environment as reported at the beginning of Section III-B3. Survived RPs are then concurrently considered by classifiers **C2**, **C3**, **C4** and **C5**, which finally return at maximum 4 different candidates, one for each classifier, to predict the new position of the person. At this point, we have two possibilities:

1) At least three classifiers among **C2**, **C3**, **C4** and **C5** agree on the same RP v_j. In this case, the person is located at v_j. Then, the probabilistic graph model is used only to decide if generating the rhythmic stimuli or not. The rhythmic stimuli is provided only in two cases: when $v_j \in V_r$, and when $v_j \in V_{ar}$ but the movement direction perceived by the smartphone goes towards an RP adjacent to v_j belonging to the risky set V_r.
2) When there is no agreement among the classifiers, given that the person was located in v_i at time t, the probability of the edges outgoing from v_i are temporarily updated according to the movement direction perceived by the smartphone, as in Section III-B4. Then, the system computes the shortest paths from v_i to each of the RP returned by **C2**, **C3**, **C4** and **C5**. The RP belonging to the highest probability path is finally selected as new location of the person. In case there is still a tie, the system locates the person at the nearest RP toward the movement direction perceived by the smartphone.

IV. EXPERIMENTAL RESULTS

This section presents the outcomes of an experimental campaign aimed at assessing the performance of the proposed approach. As a first observation, tests were performed with different types of smartphones and different users, as it is reported in Table II. The sampling frequencies relevant to the magnetic field and to RSSI measurements from BLE beacon devices are not shown in the table, as they are the same for all the devices. Specifically, the magnetic vector sampling frequency is ≥ 30 Hz, while the RSSI measurement frequency from BLE devices is ≈ 10 Hz.

The proposed system has been tested in three private indoor home environments, where, generally, a PD patient spends most of his/her time. In the initial fingerprinting phase we associated an RP (graph model vertex) to each risky position, such as doorways, stairs, floor pattern changes, etc.

TABLE II
SMARTPHONE AND USER CHARACTERISTICS

Name	Operating System	User height (ID)	AP_RSSI_{freq}
Samsung S7 Edge	Android 7.1.1	1.95 m (1)	$\approx 1Hz$
Nexus 5	Android 5.0.1	1.95 m (1)	$\approx 3Hz$
Huawei P10 Lite	Android 7.1.1	1.75 m (2)	$\approx 1Hz$
One Plus Three	Android 7.1.1	1.70 m (3)	$\approx 1Hz$
Huawei P8 Lite	Android 5.0.1	1.75 m (2)	$\approx 3Hz$

TABLE III
ACCURACY OF THE PROPOSED LOCALIZATION APPROACH

Environment	Number RPs	Our Approach (min,max)	InDoorAtlas (min,max)
Indoor (H_1)	14	$1.5m$, $1.5m$	$1m$, $8m$
Indoor (H_2)	12	$1.5m$, $1.5m$	$1m$, $8m$
Indoor (H_3)	17	$1.5m$, $1.5m$	$1m$, $8m$

a) Accuracy of the localization: In this experimental campaign we mainly evaluated the performance of the proposed localization method in terms of *absolute accuracy*, defined as the distance in meters between the real and the estimated position. The outcomes of our experiments are reported in Table III. In particular, per each environment, we may observe the number of RPs, and, in the third column, the accuracy achieved by the proposed localization approach. In all the tests we carried out, our localization system has been able to correctly recognize the risky RPs, with an absolute accuracy of 1.5m. As a further note, through the use of the probabilistic graph model the system computes also the likelihood of the user continuing to move in the direction of the risky area or turning towards a non-risky area, based on the movement direction. This allows reducing the number of unneeded stimuli when the user moves to the opposite direction with respect to (or tangent to) the risky area.

To further validate the proposed approach, the last column of Table III compares the obtained outcomes with the results achieved by using the commercial InDoorAtlas platform [15]. During all the tests we have carried out, we have observed that InDoorAtlas tends to provide a better accuracy than our approach in terms of minimum absolute accuracy (1 meter vs. 1.5 meters), as can be observed in Table III. However, the comparison with the maximum absolute accuracy (8 meters vs. 1.5 meters) revealed that InDoorAtlas is actually unsuitable for the target problem of generating rhythmic stimuli for PD patients when they approach a risky area.

Furthermore, we also observed that InDoorAtlas is very sensitive to particular movements, especially in areas hardly recognizable or not previously mapped by an RP. Particularly, in the mentioned context of PD patients, where the type of movements (short step distance at high frequency) are different from those of a healthy person (greater step distance at lower frequency), dependence on acceleration measures may become a significant source of error.

b) Energy consumption and on-device computation: The comparison between our system and InDoorAtlas let us draw some considerations about energy consumption. Indeed, we noticed that the battery consumption on the used smartphones for one hour of usage with the proposed localization system has been on average 12% of total battery charge (≈3500 joule). Conversely, with InDoorAtlas the average battery consumption for one hour of tests was 15% (≈4400 joule). Such a difference can be attributed mainly to the higher utilization of the internal sensors needed by InDoorAtlas with respect to our approach. Furthermore, we would like to emphasize that in our approach, the localization can be executed directly on the smartphone. This is because, due to the small number of RPs we need to detect a risky area, the memory occupancy for k-NN classifier is limited. The possibility of running the localization algorithm directly on the smartphone eliminates the need of an Internet connection and thus of any communication latency with a cloud server.

V. CONCLUSIONS

The paper described a low–cost localization system designed to help PD patients mitigating the effects of FoG episodes frequently happening when they approach, for example, doorways, stairs, and narrowing spaces. Experimental campaigns have shown that this approach is able to detect users in the vicinity of a risky area with an absolute accuracy of 1.5 meters.

REFERENCES

[1] M. D. Latt *et al.*, "Clinical and physiological assessments for elucidating falls risk in parkinson's disease," *Movement Disorders*, vol. 24, no. 9, pp. 1280–1289, 2009.

[2] P. Lamberti *et al.*, "Freezing gait in Parkinson's disease," *Eur. Neurol.*, vol. 38, no. 4, pp. 297–301, 1997.

[3] B. R. Bloem *et al.*, "Falls and freezing of gait in Parkinson's disease: a review of two interconnected, episodic phenomena," *Mov. Disord.*, vol. 19, no. 8, pp. 871–884, Aug 2004.

[4] A. L. S. de Lima *et al.*, "Freezing of gait and fall detection in parkinson's's disease using wearable sensors: a systematic review," *Journal of neurology*, vol. 264, no. 8, pp. 1642–1654, 2017.

[5] S. Mazilu *et al.*, "A wearable assistant for gait training for parkinson's disease with freezing of gait in out-of-the-lab environments," *ACM Trans. on Interactive Intelligent Systems*, vol. 5, no. 1, p. 5, 2015.

[6] L. Palmerini *et al.*, "Identification of characteristic motor patterns preceding freezing of gait in parkinson's disease using wearable sensors," *Frontiers in neurology*, vol. 8, p. 394, 2017.

[7] P. Bahl *et al.*, "Radar: An in-building rf-based user location and tracking system," in *INFOCOM 2000. Nineteenth Annual Joint Conference of the IEEE Computer and Communications Societies. Proceedings. IEEE*, vol. 2. Ieee, 2000, pp. 775–784.

[8] N. Alsindi *et al.*, "Cooperative localization bounds for indoor ultra-wideband wireless sensor networks," *EURASIP Journal on Advances in Signal Processing*, vol. 2008, p. 125, 2008.

[9] R. Want *et al.*, "The active badge location system," *ACM Transactions on Information Systems (TOIS)*, vol. 10, no. 1, pp. 91–102, 1992.

[10] Z. Sun *et al.*, "Pandaa: physical arrangement detection of networked devices through ambient-sound awareness," in *Proceedings of the 13th international conference on Ubiquitous computing*. ACM, 2011, pp. 425–434.

[11] Y.-S. Kuo *et al.*, "Luxapose: Indoor positioning with mobile phones and visible light," in *Proceedings of the 20th annual international conference on Mobile computing and networking*. ACM, 2014, pp. 447–458.

[12] F. Demrozi *et al.*, "A graph-based approach for mobile localization exploiting real and virtual landmarks," in *Proceedings of the IFIP/IEEE International Conference on Very Large Scale Integration (VLSI-SoC)*, 10 2018.

[13] M. Sauter, *From GSM to LTE: an introduction to mobile networks and mobile broadband*. John Wiley & Sons, 2010.

[14] A. Khalajmehrabadi *et al.*, "Modern wlan fingerprinting indoor positioning methods and deployment challenges," *IEEE Communications Surveys & Tutorials*, 2017.

[15] L. IndoorAtlas, "Ambient magnetic field-based indoor location technology: Bringing the compass to the next level," *IndoorAtlas Ltd*, 2012.

[16] I. B. Mohamad *et al.*, "Standardization and its effects on k-means clustering algorithm," *Research Journal of Applied Sciences, Engineering and Technology*, vol. 6, no. 17, pp. 3299–3303, 2013.

[17] N. M. Nasrabadi, "Pattern recognition and machine learning," *Journal of electronic imaging*, vol. 16, no. 4, p. 049901, 2007.

[18] J. Hausdorff *et al.*, "Rhythmic auditory stimulation modulates gait variability in parkinson's disease," *Eur J Neurosci.*, vol. 26, pp. 2369–2375, 2007.